



# The hydrogenation/dehydrogenation activity of supported Ni catalysts and their effect on hexitols selectivity in hydrolytic hydrogenation of cellulose



Guanfeng Liang<sup>a,b,c</sup>, Limin He<sup>a,b,c</sup>, Haiyang Cheng<sup>a,b</sup>, Wei Li<sup>a,b</sup>, Xiaoru Li<sup>a,b,c</sup>, Chao Zhang<sup>a,b</sup>, Yancun Yu<sup>a,b</sup>, Fengyu Zhao<sup>a,b,\*</sup>

<sup>a</sup>State Key Laboratory of Electroanalytical Chemistry, Changchun Institute of Applied Chemistry, Chinese Academy of Sciences, Changchun 130022, PR China

<sup>b</sup>Laboratory of Green Chemistry and Process, Changchun Institute of Applied Chemistry, Chinese Academy of Sciences, Changchun 130022, PR China

<sup>c</sup>University of Chinese Academy of Sciences, Beijing 100049, PR China

## ARTICLE INFO

### Article history:

Received 4 July 2013

Revised 24 October 2013

Accepted 29 October 2013

Available online 3 December 2013

### Keywords:

Hydrogenation/dehydrogenation

Ni catalysts

Cellulose hydrogenation

Hexitols productivity

## ABSTRACT

A series of Ni catalysts were prepared with various supports (ZSM-5, Al<sub>2</sub>O<sub>3</sub>, SiO<sub>2</sub>, bentonite, TiO<sub>2</sub>, and kieselguhr) and their catalytic properties were investigated for the hydrogenation of cellobiose and glucose, the reaction intermediates of cellulose hydrolysis in hot-compressed water, in order to elucidate the key factors to control the hexitols selectivity in the hydrolytic hydrogenation of cellulose. For the hydrogenation of cellobiose, hexitols were produced with a selectivity above 82% over Ni/ZSM-5, but the other checked Ni catalysts produced large amount of glycerol, ethylene glycol, and propanediol, and the product distribution strikingly depended on the catalysts used. On the basis of kinetic experiments, it was the hydrogenation/dehydrogenation ability of Ni catalyst that played a critical role in controlling hexitols selectivity. High hydrogenation and inferior dehydrogenation activity of Ni catalysts were essential for obtaining high yield of hexitols in the hydrolytic hydrogenation of cellulose. The synergistic effect of Ni active species and acid–base sites was proposed to accelerate the dehydrogenation of sorbitol and thus reducing the yield of hexitols.

© 2013 Elsevier Inc. All rights reserved.

## 1. Introduction

Cellulose is one of the most abundant forms of biomass on the earth, and the transformation of cellulose to fuels and chemicals has triggered more and more intense worldwide research interest. The efficient conversion of cellulose into target products through various catalytic processes has been regarded as one viable way to reduce the CO<sub>2</sub> emission and alleviate the energy crisis [1]. Chemical processes such as hydrolysis, gasification, and pyrolysis have been investigated for converting cellulosic biomass into chemicals. Specifically, one-pot catalytic conversion of cellulose into chemicals of polyols, ethylene glycol, and alkyl glycosides was developed, which is considered to be one of the most efficient methods [2–4]. So far, the hydrolytic hydrogenation of cellulose into polyols via one-pot method in hot-compressed water is a promising approach for its greenness and energy efficiency compared to other primary conversion processes. Fukuoka et al. firstly

\* Corresponding author at: State Key Laboratory of Electroanalytical Chemistry, Changchun Institute of Applied Chemistry, Chinese Academy of Sciences, Changchun 130022, PR China.

E-mail address: [zhaofy@ciac.ac.cn](mailto:zhaofy@ciac.ac.cn) (F. Zhao).

investigated the conversion of cellulose into sugar alcohols over supported noble metal catalysts and about 31% yield of hexitols (sorbitol and mannitol) was obtained by using Pt/Al<sub>2</sub>O<sub>3</sub> catalyst within 24 h at 190 °C [5]. Liu et al. demonstrated that about 30% yield of sorbitol was obtained at 85.5% conversion of cellulose on supported Ru clusters within 30 min at 245 °C [6]. Various subsequent studies showed that Ru catalysts were highly efficient hydrogenation catalysts on cellulose conversion [6–10]. For example, Palkovits et al. demonstrated the introduction of dilute mineral acids could effectively promote the catalytic performance of supported Pt, Pd, and Ru catalysts on cellulose conversion, and their further research showed that the yield of sugar alcohols increased with combining heteropoly acids and Ru/C [9,11]. Sels et al. presented the combination of Ru-loaded zeolites and trace amounts of mineral acid could produce >90% yield of hexitols with complete cellulose conversion at mild conditions [8,12,13]. Wang et al. demonstrated the abundant acidic groups and larger Ru particles on Ru/CNTs could favor high yield of hexitols [7,14]. In our previous study, isosorbide could be obtained with a 50% yield from hydrogenation of microcrystalline cellulose over Ru/C catalyst with dilute hydrochloric acid at 215 °C and 6.0 MPa H<sub>2</sub> for 6 h [15]. Very recently, Sels et al. reported a more efficient way in isosorbide

production by using  $\text{H}_4\text{SiW}_{12}\text{O}_{40}$  and Ru/C, and 63% yield of isosorbide could be obtained from the fibrillar cellulose within 1 h [16].

All the above results are really promising; nevertheless, the selective hydrolytic hydrogenation of cellulose into polyols is still a big challenge. One significant disadvantage is the use of large amount of noble metal catalyst, making those approaches too expensive for the large-scale application in industry. Recently, attention is drawn to the non-noble metal catalysts, including Ni, Cu, and tungsten carbide catalysts because of the fast turnover rates, availability, and low cost. Zhang et al. studied the catalytic performance of Ni-promoted tungsten catalysts on cellulose hydrogenation; notably, ethylene glycol (EG) was obtained with 61% yield at 245 °C [17]. In their following research, tungsten carbide on mesoporous carbon (MC) and Ni-W/SBA-15 were demonstrated to be also effective for catalyzing cellulose and produced EG with the highest yield of 72.9% [18,19]. Conventional Ni-based catalysts have always been used as effective catalysts for aqueous-phase hydrogenolysis of sorbitol to produce glycerol, ethylene glycol, and propanediol. Unfortunately, supported Ni catalysts exhibited inferior performance in the transformation of cellulose into sorbitol. The attempts to increase activity and selectivity of Ni-based catalysts for the cellulose hydrogenation still encounter great difficulties. Therefore, the modified Ni-based catalysts are designed to promote the yield of sorbitol by suppressing the subsequent hydrogenolysis reaction. Sels et al. obtained 50% yield of sorbitol at 92% conversion of cellulose over the reshaped Ni particles on carbon nanofibers [20], their further study indicated that the metal active sites and the acidic functional group on Ni/CNFs should be properly balanced, and the 7.5 wt% Ni/CNFs with a relatively high amount of Ni surface atoms ( $26.9 \text{ mmol}_{\text{cat}}^{-1}$ ) and low density of Brønsted acid sites ( $0.02 \text{ mmol}_{\text{H}^+} \text{ g}^{-1}$ ) gave 76% yield of hexitols at a cellulose conversion of 93% [21]. Zhang et al. reported that nickel phosphides supported on activated carbon and  $\text{SiO}_2$  were effective for conversion of cellulose to sorbitol, and about 48% yield of sorbitol was reached at complete conversion [22]. Moreover, they developed various Ni-based bimetallic catalysts using mesoporous carbon (MC) as support; more recently, nearly 60% yield of sorbitol was obtained over the Ir–Ni/MC catalyst [23]. In addition, they also developed a binary catalyst system composed of tungstic acid and Raney Ni which produced 65% of ethylene glycol [24]. 20% Ni/ZnO was reported to be one of the most effective catalysts among a series of the supported Ni catalysts, with it 70% yield of glycols (1,2-propanediol, ethylene glycol, 1,2-butanediol, and 1,2-hexanediol), which was obtained at complete cellulose conversion [25]. The above studies suggested that the support has a significant effect on the product selectivity in cellulose hydrogenation over the Ni based catalysts. However, the real role of Ni particles on the hydrolytic hydrogenation was still unclear as the whole process involved hydrolysis, hydrogenation, and hydrogenolysis steps was rarely studied. Specially, the relationship between the activity and the nature of hydrogenation catalysts in conversion of cellulose was still elusive.

For production of hexitols, a desired Ni catalyst should promote the hydrogenation of C=O bond in aldose or polysaccharide, but retard the further hydrogenolysis of hexitols or parallel reactions including aqueous phase reforming of polyols. We previously reported that Ni/ZSM-5 could efficiently catalyze cellulose into hexitol with about 91% selectivity at 48.6% conversion at 230 °C [26]. We demonstrated the Ni/ZSM-5 catalyst with petaloid-like nickel particles could not only favor the hydrogenation of the glucose formed, but also suppress the further hydrogenolysis of sorbitol, leading to a high yield of sorbitol. However, there is still little knowledge about the effect of the Ni catalysts on the conversion of cellulose to sorbitol. Therefore, it is essential to figure out the key factors that determine the production of hexitol. In this paper, the basic reaction steps in the hydrolytic hydrogenation of

microcrystalline cellulose over Ni catalysts, including the hydrogenation of cellobiose and glucose, as well as the dehydrogenation of sorbitol, were discussed in order to figure out the correlation between the catalytic performance and the nature of the catalyst. The kinetic study demonstrated that the hydrogenation/dehydrogenation ability of Ni catalysts had significant influence on the catalytic activity and selectivity of Ni catalysts in converting cellulose into hexitols.

## 2. Experimental

### 2.1. Materials

Microcrystalline cellulose (relative crystallinity of about 74.6%, Alfa Aesar) was dried at 70 °C for 24 h before use.  $\text{Ni}(\text{NO}_3)_2 \cdot 9\text{H}_2\text{O}$  (AR) was purchased from Sinopharm Chemical Reagent,  $\text{SiO}_2$  (Sigma–Aldrich),  $\text{TiO}_2$  (Sigma–Aldrich),  $\gamma\text{-Al}_2\text{O}_3$ , bentonite, and kieselguhr (Sinopharm Chemical Reagent) were used as received. ZSM-5 (NKF-5, H type, Si/Al = 25, 38, 50), HY, and USHY were purchased from the Catalyst Plant of Nankai University. Nano CuO was obtained from Aladdin.

### 2.2. Catalyst preparation

The supported Ni catalysts were prepared by a modified incipient impregnation method. In detail, a series of supports ( $\text{Al}_2\text{O}_3$ ,  $\text{SiO}_2$ , ZSM-5, bentonite, kieselguhr, and  $\text{TiO}_2$ ) were immersed in an aqueous  $\text{Ni}(\text{NO}_3)_2$  solution with a certain concentration at room temperature. The mixture was treated under ultrasonic condition for 0.5 h and the solid suspension was formed. Then, the solid suspension was dried at 70 °C with stirring. During this process, the solvent was evaporated slowly until the solid suspension was dried to powder again. This process will take about 3 h; after that, the mixture was vacuum dried at 60 °C for 12 h, followed by calcinations under Ar atmosphere at 450 °C for 2 h with heating rate of  $5 \text{ }^\circ\text{C min}^{-1}$ . Prior to reaction or characterization, all the catalysts were reduced under  $\text{H}_2$  atmosphere for 2 h at appropriate temperatures with a heating rate of  $5 \text{ }^\circ\text{C min}^{-1}$ .

### 2.3. Catalyst characterization

Powder X-ray diffraction of the samples was recorded on a Bruker D8 Advance X-ray diffractometer with a Cu K $\alpha$  source ( $\lambda = 0.154 \text{ nm}$ ) in the  $2\theta$  range 10–80° with a scan speed of  $10^\circ \text{ min}^{-1}$ .

$\text{H}_2$ -temperature-programmed reduction ( $\text{H}_2$ -TPR),  $\text{H}_2$ -temperature-programmed desorption ( $\text{H}_2$ -TPD), and  $\text{NH}_3$ -temperature-programmed desorption ( $\text{NH}_3$ -TPD) were conducted on a Tianjin XQ TP-5080 chemisorption instrument with a thermal conductivity detector (TCD). As for  $\text{H}_2$ -TPR, 30 mg of fresh catalyst was loaded into a quartz reactor. Before  $\text{H}_2$ -TPR, the catalysts were heated at 150 °C for 30 min in nitrogen and then cooled to room temperature. The sample was reduced in a 10%  $\text{H}_2/\text{N}_2$  flow with a heating rate of  $10 \text{ K min}^{-1}$ . The effluent gas was analyzed with a thermal conduction detector (TCD). As for the  $\text{H}_2$ -temperature-programmed desorption, 100 mg of each catalyst was loaded into a quartz reactor and then reduced with a  $\text{H}_2$  flow at appropriate temperature. After reduction, the reactor was cooled down to room temperature and then the catalyst sample was maintained under  $\text{H}_2$  flow for 30 min. Following the desorption step, the reactor was flushed with  $\text{N}_2$  for 2 h to reach a stable background. At last,  $\text{H}_2$ -TPD was carried out with  $\text{N}_2$  at a flow rate of  $30 \text{ mL min}^{-1}$  and a temperature ramp rate of  $10 \text{ }^\circ\text{C min}^{-1}$ . The process of  $\text{NH}_3$ -TPD was same as that of  $\text{H}_2$ -TPD.

## 2.4. Catalytic experiments

All the catalysts were pre-reduced by  $H_2$  for 2 h at appropriate temperatures with heating rate of  $5\text{ }^\circ\text{C min}^{-1}$  before reaction. In a standard experiment, the reduced catalyst was transferred from the quartz tube to a 30 mL Teflon-lined stainless steel autoclave (30 i.d  $\times$  45 mm) with 10 mL water by a glass catheter, and then, the substrate was loaded into the reactor. The reactor was flushed with  $H_2$  for three times and then pressurized with 4 MPa  $H_2$  (RT). After being heated to the desired temperature with stirring at a low agitating rate, the reaction was started with stirring at a rate of 1200 rpm. After reaction, the products were centrifuged to separate the solid. The solid was dried at  $70\text{ }^\circ\text{C}$  overnight and weighted. The cellulose conversion was calculated by weight difference in the solid substrates before and after reaction.

## 2.5. Product analysis

The products were analyzed by GC/MS after the liquid products being acetylated, and more than 15 polyols were detected, among which sorbitol (or mannitol, GC/MS could not identify these two isomers), glycerol, ethylene glycol, and propanediol are the main products, with accompanied by minor byproducts including sorbitan  $C_4$  and  $C_5$  polyols, etc. All those minor byproducts have complex isomers and most of them are with peak determination quality less than 50%, so it is really difficult to identify the structure for each of the minor byproducts.

The products in the aqueous solution were firstly identified by GC/MS (Agilent 5975/6890N) with a HP-5 column (30 m  $\times$  0.25  $\mu\text{m}$   $\times$  0.25 mm i.d) after acetylation. Quantification of the each polyol was conducted by using HPLC with external standard method. The products were analyzed by a HPLC system (Shimadzu LC-20AB) equipped with RI detector (Shimadzu RID-10A) and a Aminex HPX-87H column (Bio-Rad, 300  $\times$  7.8 mm), using 5 mM  $H_2SO_4$  as eluent with a flow rate of  $0.7\text{ mL min}^{-1}$  at  $60\text{ }^\circ\text{C}$ . The  $H_2$  produced in the dehydrogenation of sorbitol was quantified by GC (Shimadzu GC-14C) equipped with packed column with a TCD detector.

The HPLC analysis also showed that sorbitol (mannitol), glycerol, ethylene glycol, and propanediol were the main liquid products. The quantification of the liquid products was conducted by a HPLC system based on calibration curves of the stand compounds.

The yield of the product is calculated by the moles of carbon in product divided by the moles of carbon in cellulose. The conversion of cellulose was calculated with the initial weight of cellulose, and the catalyst divided by the residual solid weight after reaction. The carbon efficiency was calculated by the ratio of moles of carbon in the polyols to those in the substrate.

## 3. Results and discussion

### 3.1. Ni catalysts and their physical properties

The hydrolytic hydrogenation of cellulose is starting with the hydrolysis to produce glucose and then the glucose hydrogenates directly to hexitols (sorbitol and mannitol) over the catalyst. From this point of view, the hydrogenation activity of the catalyst is important for obtaining high yield of hexitols. The specific surface area of metal particles, metal dispersion, and crystallite sizes is always considered to be the key influencing factor for hydrogenation activity [13–16]. In order to figure out the key factors for determining the production of hexitol over Ni catalysts in hydrolytic hydrogenation of cellulose, the above parameters of several Ni catalysts have been examined by  $H_2$ -TPD,  $NH_3$ -TPD, and XRD analysis, and

the results are summarized in Table 1 (The patterns are shown in Supplementary information.). The most catalysts presented comparable specific surface area and nickel dispersion except for Ni/bentonite, and it has much lower specific surface area due to the large Ni particles.

The acidity is always related to the hydrolysis rate of cellulose and the selectivity for the hexitols in hydrolytic hydrogenation of cellulose. Herein, the  $NH_3$ -TPD was examined for all the catalysts (Fig. S2), and the peak area at  $95\text{ }^\circ\text{C}$  on Ni/ $Al_2O_3$  was assigned as 1.0, based on which the values of surface acidity for other samples were calculated. The peaks at a temperature range of  $50$ – $250\text{ }^\circ\text{C}$  and  $400$ – $650\text{ }^\circ\text{C}$  were assigned to the weak and strong acid sites, respectively. The surface acidity of the Ni catalysts was originated from the acidity of the support, which was quite different from each other. Ni/ZSM-5 had the highest amount of strong acidic sites among the Ni catalysts, and Ni/ $TiO_2$  gave two kinds of weak acid sites at low temperatures. One single kind of acidic site was shown for Ni/ $SiO_2$ , while no acidic site was observed on Ni/kieselguhr.

### 3.2. The factors effect on hexitols productivity

#### 3.2.1. Surface acidity

Fukuoka and Dhepe firstly reported the direct conversion of cellulose into sugar alcohols (sorbitol and mannitol) in water with a series of bifunctional supported metal catalysts, wherein the support acted as acidic sites for hydrolysis and the metal center worked as active sites for hydrogenation [5]. The “bifunctional catalysis” concept was widely accepted, and many promising results are reported by combining metal active sites with solid acids. It should be noted that all these studies were conducted at low temperatures ( $150$ – $200\text{ }^\circ\text{C}$ ), wherein the hydrolysis rate was quite low. Moreover, the hydrolysis rate did not correspond well with the strength of the acid [5]. Herein, we revealed a very different hydrolysis behavior. Fig. 1 shows the conversion of cellulose as a function of time over Ru/C and Ni/ZSM-5 at  $240\text{ }^\circ\text{C}$ . ZSM-5 is known as an acidic support with large amount of strong acidic sites, while activated carbon is an inert support with few acidic function groups. Even though both the catalysts of Ru/C and Ni/ZSM-5 have totally different metal active sites or supports, they presented the similar trend in cellulose conversion. In our preliminary research, we found that all the Ni catalysts with various supports gave similar conversion at the identical reaction conditions [26]. Therefore, we can conclude that the surface acidity of supports did not affect on the hydrolysis step at elevated temperatures. The acidic sites of the support indeed promoted the hydrolysis of cellulose in some extent at low temperatures ( $150$ – $200\text{ }^\circ\text{C}$ ) at which the hydrolysis rate was quite slow; it is in agreement to the literature [5,28]. However, such promotion was negligible at the high temperatures when the hydrolysis rate was fast.

#### 3.2.2. Temperature

Table 2 summarizes the hydrogenation of microcrystalline cellulose in neutral water, in which the results based on ball-milled cellulose or with addition of acids are excluded. We could find that the hydrolysis rate was sensitive to temperature, and it was quite slow at the temperatures below  $200\text{ }^\circ\text{C}$ , but increased greatly with increasing temperature for all the catalysts reported, which could be explained by the large activation energy for hydrolysis. It has been proven that the activation energy for cellulose hydrolysis is around  $172$ – $189\text{ kJ mol}^{-1}$  in batch reactors with acids [29], indicating that the hydrolysis rate could be accelerated greatly by increasing reaction temperature. The hydrolysis rate ( $34.2\text{ mg mL}^{-1}\text{ h}^{-1}$ ) at  $245\text{ }^\circ\text{C}$  (Table 2, line 8) was at least 170 times larger than those ( $0.15$ – $0.2\text{ mg mL}^{-1}\text{ h}^{-1}$ ) at  $190\text{ }^\circ\text{C}$  (Table 2, line 3 and 4), which was independent of the catalysts used. Therefore, the elevated temperature was very essential for the fast hydrolysis of cellulose.

**Table 1**  
Some properties of the supported nickel catalysts.

Catalyst	Acid sites distribution based on NH <sub>3</sub> -TPD data <sup>a</sup>			Nickel particle size (nm)		SA <sub>Ni</sub> <sup>d</sup> (m <sup>2</sup> g <sup>-1</sup> )	Dispersion <sup>e</sup> (%)
	Weak	Strong	Total	XRD <sup>b</sup>	H <sub>2</sub> -TPD <sup>c</sup>		
Ni/ZSM-5	0.84	1.13	1.97	21.0	16.9	39.89	5.9
Ni/Al <sub>2</sub> O <sub>3</sub>	1.00	0.26	1.26	24.6	19.2	35.06	5.2
Ni/SiO <sub>2</sub>	0.58	0.05	0.63	12.7	15.6	42.91	6.4
Ni/bentonite	0.24	0.43	0.67	26.1	35.9	18.75	2.8
Ni/TiO <sub>2</sub>	0.31	0.14	0.45	14.8	17.8	37.71	5.6
Ni/kieselguhr	NA	NA	NA	17.0	NA <sup>f</sup>	NA	NA

<sup>a</sup> The data were calculated by the peak area based on a standard sample of Ni/Al<sub>2</sub>O<sub>3</sub>, in which the peak area at 95 °C is assigned as 1.0.

<sup>b</sup> The data were obtained according to Scherrer–Warren equation.

<sup>c</sup> The instrument was calibrated by nano CuO.

<sup>d</sup> Ni metal-specific surface area (SA<sub>Ni</sub>) was calculated based on the amount of hydrogen desorption from H<sub>2</sub>-TPD [24].

<sup>e</sup> Based on H<sub>2</sub>-TPD data.

<sup>f</sup> NA: the data were not available.

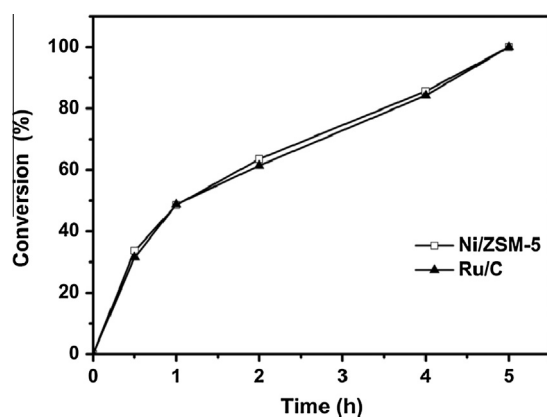


**Fig. 1.** The cellulose conversion over Ni/ZSM-5 and Ru/C as a function of time. Reaction conditions: 240 °C, 10 mL H<sub>2</sub>O, 4.0 MPa H<sub>2</sub>, microcrystalline cellulose 0.2 g, Ni/ZSM-5 (17 wt% Ni) 100 mg, Ru/C (5 wt% Ru) 10 mg.

On the other hand, the hydrolytic hydrogenation of cellulose is an integrated process including depolymerization, hydrolysis, and hydrogenation. These steps are always accompanied with several side reactions (Fig. 2), such as glucose degradation, hydrogenolysis, aqueous phase reforming, and water–gas shift reaction. These side reactions are usually negligible at low temperature (<200 °C), but became obvious at high temperature (>230 °C), resulting in a complex product distribution. For example, more than 90% yield of hexitols was readily obtained over Ru/C at low temperature (<200 °C) in previous reports [8,12,13], when the temperature increased to 245 °C, the hexitols yield declined to about 40% [6]. Overall, the yield of hexitols at elevated temperature was related to the following two aspects (1) over the inferior-activity nickel

catalyst, the glucose decomposed seriously to complex products via degradation and condensation before it was hydrogenated to hexitols; (2) Over the high-activity nickel catalyst, glucose was hydrogenated to hexitols immediately before decomposition, and the formed hexitols might subsequently suffer serious hydrogenolysis to yield smaller molecular polyols. The possible reaction pathway for the hydrolytic hydrogenation of cellulose over Ni catalysts at elevated temperatures is shown in Fig. 2, which is quite different from that at low temperatures. The hydrogenation activity of the catalyst was the primary factor for obtaining hexitols at low temperature. However, the hexitols production at evaluated temperature is not only related to the hydrogenation activity, several side reactions catalyzed by hydrogenation catalysts are involved in controlling the hexitols yield. So it is unreasonable to evaluate the hydrogenation activity of a catalyst by the yield of hexitols only at high temperature. Therefore, the hexitols productivity is listed in Table 2 to evaluate the efficiency of the individual catalytic system. By comparison of the hexitols productivity at different temperatures, we deduced that both the fast hydrolysis rate and high hexitols selectivity are required for high productivity of hexitols.

### 3.2.3. Feedstock

Cellobiose, a glucose dimer connected by 1,4-β-glycosidic bond, is considered to be the simplest model molecule of cellulose, and glucose is the final product of cellulose hydrolysis. To investigate the hydrogenation of these two key intermediates is of great importance in elucidating the reaction pathway and the different hydrogenation activities of Ni catalysts. In the previous studies, the supported nickel catalysts showed excellent activity on the hydrogenation of monosaccharides, oligo- and polysaccharides (sucrose and starch), over which hexitols were obtained as major products with high selectivity at mild reaction condition (<150 °C) [33–35]. In the case of cellulose hydrogenation, elevated

**Table 2**  
The results for the hydrolytic hydrogenation of microcrystalline cellulose in neutral water in literature.

Catalyst	Conditions	Conversion (%)	Hexitols yield (%)	Hydrolysis rate <sup>a</sup> (mg mL <sup>-1</sup> h <sup>-1</sup> )	Hexitols productivity <sup>b</sup> (mg mL <sup>-1</sup> h <sup>-1</sup> )	Ref.
Ru/CNT	458 K, 5.0 MPa H <sub>2</sub> , 24 h	NA	40	–	0.13	[14]
Pt/γ-Al <sub>2</sub> O <sub>3</sub>	463 K, 5.0 MPa H <sub>2</sub> , 24 h	NA	31.1	–	0.10	[5]
Pt/γ-Al <sub>2</sub> O <sub>3</sub>	463 K, 5.0 MPa H <sub>2</sub> , 24 h	60	15	0.2	0.07	[30]
2.0% Pt/BP2000	463 K, 5.0 MPa H <sub>2</sub> , 24 h	66	42	0.15	0.09	[31]
16% Ni <sub>2</sub> P/AC	498 K, 6.0 MPa H <sub>2</sub> , 1.5 h	100	53	6.7	3.55	[22]
3.0% Ni/CNF	503 K, 4.0 MPa H <sub>2</sub> , 4 h	93.9	27.6	4.7	1.38	[21]
Ni/ZSM-5	513 K, 4.0 MPa H <sub>2</sub> , 4 h	85.5	58.2	5.0	2.48	[27]
Ru/C	518 K, 6.0 MPa H <sub>2</sub> , 0.5 h	85.5	39.3	34.2	13.4	[6]
Ni/W/SiO <sub>2</sub> -Al <sub>2</sub> O <sub>3</sub>	518 K, 6.0 MPa H <sub>2</sub> , 2 h	92	28.4 <sup>c</sup>	7.7	2.38	[32]

<sup>a</sup> The hydrolysis rate is calculated by the weight of reacted cellulose per mL per hour.

<sup>b</sup> Hexitols productivity is calculated by the weight of hexitol produced per mL per hour.

<sup>c</sup> The products were EG and PDO.



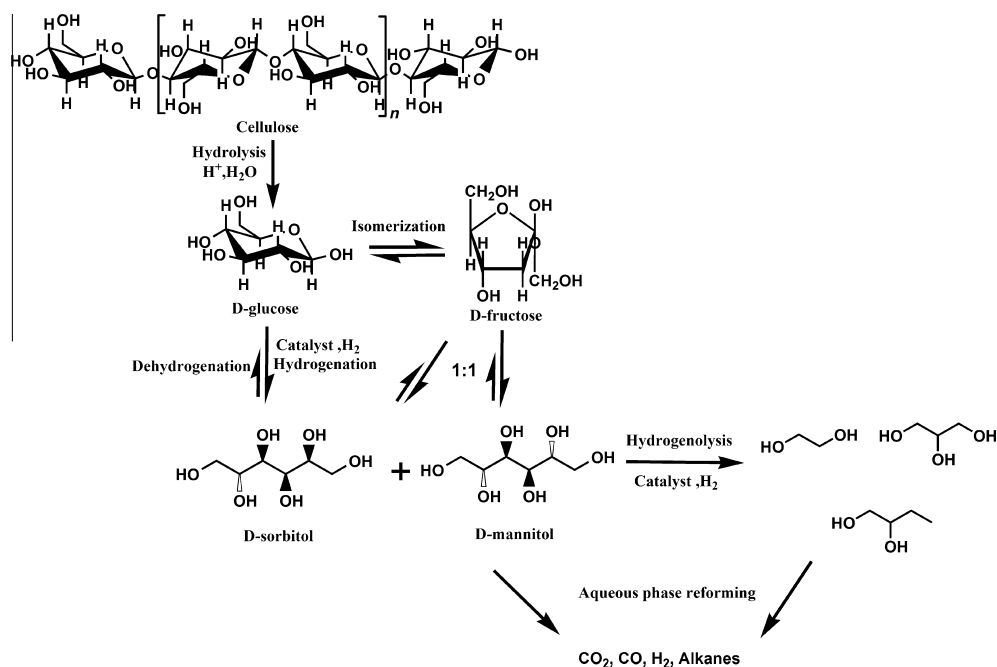


Fig. 2. The proposed reaction pathways for the transformation of cellulose over Ni catalysts.

temperature (>230 °C) was required for the fast hydrolysis of cellulose. The hexitols yield decreased accompanied by the formation of large amount of C<sub>3</sub>–C<sub>2</sub> polyols at the elevated temperature [26]. In this work, the hydrogenation of cellobiose and glucose over Ni catalysts were conducted at the identical conditions to that in cellulose hydrogenation in order to figure out the real controlling factors for the product distribution in the conversion of cellulose over Ni catalysts, and the results are summarized in Tables 3 and 4. All the catalysts gave higher carbon efficiency and hexitols yield in the hydrogenation of cellobiose and glucose compared to that for microcrystalline cellulose. The product distribution in the hydrogenation of cellobiose and glucose was similar to that in the conversion of microcrystalline cellulose over all the Ni catalysts [26]. Ni/ZSM-5 showed both high carbon efficiency and hexitols yield in the hydrogenation of cellobiose and glucose, while the other Ni catalysts gave the hydrogenolysis products of glycerol, ethylene glycol, and propanediol with a low carbon efficiency. This phenomenon indicated that the nature of Ni catalysts played a critical role in the product distribution irrespective of molecular structure of the feedstock. The relation of the polyols selectivity and the nature of the support have also been discussed in the previous studies [25], but there was still no direct evidence for the correlation between surface acid–basicity of supports and the selectivity to hexitols. In general, the hydrogenation reaction occurred on the surface of nickel particles, and the reaction rate and product

selectivity depended on the nature of nickel particles and supports, so that the interaction or synergistic effect between the Ni particles and the supports should have a large effect on the catalytic performance.

### 3.3. Reaction mechanism for hexitol hydrogenolysis

#### 3.3.1. Sorbitol dehydrogenation

In our previous study, it was demonstrated that the hydrogenolysis of hexitol affected the final yield of hexitols [26]. However, the underlying mechanism for the hydrogenolysis was still indeterminate. It was often claimed that sorbitol hydrogenolysis was related to hydrogenolysis of C–C and C–O bonds, that is, direct cleavage of C–C and C–O bands by hydrogen. However, no evidence for that process has been given. According to the study reported by Liu et al., the cleavage of C–C bond was caused by retro-aldol condensation in the hydrogenolysis of xylitol [36]. If this assumption was reasonable, the unsaturated aldose/ketose must be formed by dehydrogenation of sorbitol prior to retro-aldol condensation. In this work, we first conducted the conversion of sorbitol over a series of supported Ni catalysts under N<sub>2</sub> at 250 °C for 2 h. As shown in Table 5, glucose was found in the liquid products, which was a proof for the occurrence of dehydrogenation of sorbitol. The amount of H<sub>2</sub> produced was determined by gas chromatography, and the liquid products were analyzed by liquid chromatography.

Table 3  
Results for the hydrogenation of cellobiose on supported Ni catalysts.<sup>a</sup>

Catalysts	Conversion (%)	Carbon efficiency <sup>b</sup> (%)	Yield (%)			
			Hexitols	Glycerol	EG	1,2-PDO
Ni/ZSM-5	100	87.6	82.1	2.4	1.9	1.2
Ni/Al <sub>2</sub> O <sub>3</sub>	100	67.1	28.8	21.3	6.6	10.4
Ni/SiO <sub>2</sub>	100	56.6	44.4	7.0	3.5	1.7
Ni/bentonite	100	75.9	54.5	6.7	5.1	9.6
Ni/TiO <sub>2</sub>	100	48.9	32.3	5.1	4.4	7.1
Ni/kieselguhr	100	55.8	24.5	13.5	5.2	12.6

<sup>a</sup> Reaction conditions: 240 °C, H<sub>2</sub> 4.0 MPa (RT), cellobiose 0.2 g, H<sub>2</sub>O 10 mL, 4 h, catalyst 100 mg, Ni loading is 40%.

<sup>b</sup> Carbon efficiency was calculated through the yield of polyols divided by cellobiose conversion.

**Table 4**  
Results for the hydrogenation of glucose over supported Ni catalysts.<sup>a</sup>

Catalysts	Conversion (%)	Carbon efficiency (%)	Yield (%)			
			Hexitols	Glycerol	EG	1,2-PDO
Ni/ZSM-5	98.9	84.2	76.3	3.0	2.2	1.8
Ni/Al <sub>2</sub> O <sub>3</sub>	100	56.9	19.5	12.6	6.6	18.2
Ni/SiO <sub>2</sub>	100	61.5	24.1	19.3	6.3	11.8
Ni/bentonite	100	83.1	52.0	14.3	5.2	11.6
Ni/TiO <sub>2</sub>	100	58.4	39.3	8.3	4.0	6.8
Ni/kieselguhr	98.8	56.5	30.0	9.7	4.9	11.2

<sup>a</sup> Reaction conditions was identical with that in cellobiose hydrogenation, glucose 0.2 g.

**Table 5**  
Dehydrogenation of sorbitol over supported Ni catalysts.<sup>a</sup>

Catalysts	Conversion (%)	H <sub>2</sub> (mL)	Gas (mL)	Yield (%)			
				Glycerol	EG	1,2-PDO	Glucose
Ni/ZSM-5	22.3	4.0	20.8	0.7	1.8	4.1	1.4
Ni/Al <sub>2</sub> O <sub>3</sub>	42.0	2.2	45.8	1.2	1.7	10.2	0.2
Ni/SiO <sub>2</sub>	26.3	8.1	23.4	1.1	1.8	3.6	1.3
Ni/bentonite	29.2	5.3	17.2	0.6	1.9	6.0	0.1
Ni/TiO <sub>2</sub>	18.6	2.5	16.8	0.6	1.5	4.4	0.2
Ni/kieselguhr	2.3	5.4	17.3	0.4	0.8	2.0	1.9

<sup>a</sup> Reaction conditions: 250 °C, N<sub>2</sub> 0.1 MPa (RT), sorbitol 0.5 g, H<sub>2</sub>O 10 mL, 2 h, catalyst 100 mg, Ni loading is 40%.

A certain amount of hydrogenolysis products were obtained as the major liquid products in the absence of extra H<sub>2</sub>, indicating that the formed H<sub>2</sub> directly participated in the subsequent hydrogenation of the intermediates produced from retro-aldol condensation. On the other hand, the effect of the acidity of the support may not be excluded. If sorbitol was adsorbed on the supports, it might undergo cyclodehydration reaction on the surface acid sites to form sorbitan and isosorbide. In fact, these dehydration products were produced with minor amount to be detected, indicating that the dehydration of hexitols was inhibited on the surface of catalyst. The adsorbed hexitols on the Ni catalysts were predominantly dehydrogenated to unsaturated species, rather than cyclodehydrated into sorbitan or isosorbide.

Thus, the rate of dehydrogenation could be estimated by the consumption rate of sorbitol. We compared the dehydrogenation activity of the Ni catalysts in terms of the initial conversion rate of sorbitol in N<sub>2</sub> atmosphere, and the hydrogenolysis activity was compared in terms of initial conversion rate of sorbitol in 4.0 MPa H<sub>2</sub> (conversion <15%). As shown in Fig. 3, in the case of Ni/Al<sub>2</sub>O<sub>3</sub>, Ni/SiO<sub>2</sub>, Ni/ZSM-5, and Ni/bentonite, the initial rate of hydrogenolysis was slightly lower than that of dehydrogenation, while Ni/kieselguhr and Ni/TiO<sub>2</sub> showed a reverse trend. The initial rate of sorbitol hydrogenolysis was in consistent with that of dehydrogenation for all Ni catalysts checked. For example, Ni/Al<sub>2</sub>O<sub>3</sub> gave the highest activity in dehydrogenation and also presented the highest activity in sorbitol hydrogenolysis correspondingly. By comparison, Ni/ZSM-5 and Ni/kieselguhr presented lower activity in the both hydrogenolysis and dehydrogenation. According to the above discussion, we found that the dehydrogenation step was the crucial step for the hydrogenolysis of sorbitol. We proposed that the sorbitol hydrogenolysis was started from dehydrogenation followed by retro-aldol condensation and hydrogenation. The adsorbed hexitols on the catalyst surface firstly underwent dehydrogenation to form the unsaturated adsorbed species, wherein H<sub>2</sub> was produced by the cleavage of C–H bonds. The unsaturated adsorbed species might be desorbed from the Ni metal surface to form glucose. On the other hand, it is more likely to undergo retro-aldol condensation catalyzed by the acid–base of the support and H<sup>+</sup>/OH<sup>−</sup> dissociate by hot-compressed water to give glycolaldehyde and glyceraldehyde. The glycolaldehyde and

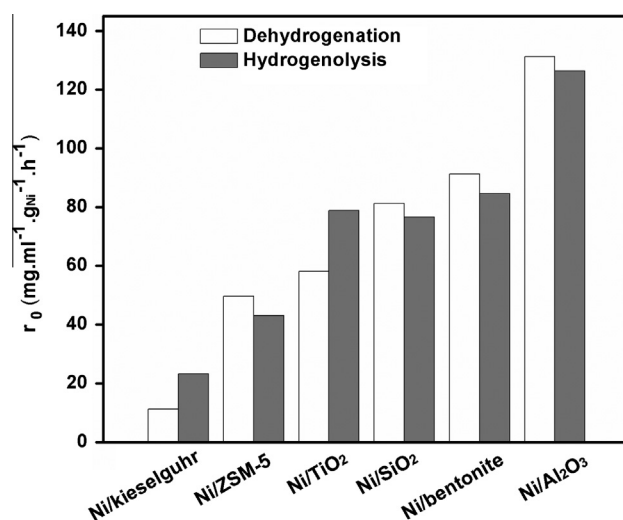


**Fig. 3.** Comparison of the initial rate for hydrogenolysis and dehydrogenation of sorbitol over various supported Ni catalysts. Reaction conditions: 240 °C, 10 mL H<sub>2</sub>O, 4.0 MPa H<sub>2</sub> (hydrogenolysis reaction, RT) or 0.1 MPa N<sub>2</sub> (dehydrogenation reaction, RT), sorbitol 0.5 g, Ni catalyst (40 wt% Ni) 100 mg, 2 h.

glyceraldehydes then were re-adsorbed on the metal surface and hydrogenated to form ethylene glycol and glycerol. The further dehydration and hydrogenation of glycerol produced propylene glycol. This deduction was further supported by the existence of C<sub>2</sub>–C<sub>3</sub> polyols in the dehydrogenation of sorbitol.

### 3.3.2. The hydrogenation/dehydrogenation activity

In the previous studies, too much attention was focused on designing the catalyst with high hydrogenation activity for guaranteeing high yield of hexitols, wherein the parameters like metal type, metal dispersion, and acidity/basicity of support are always emphasized; meanwhile, the dehydrogenation activity of the catalyst has been largely overlooked.

A comparative study on Ni/ZSM-5 and Ni/Al<sub>2</sub>O<sub>3</sub> was conducted. Ni/ZSM-5 showed the highest yield of hexitols, while Ni/Al<sub>2</sub>O<sub>3</sub> gave

low yield of hexitols in hydrogenation of microcrystalline cellulose, cellobiose, and glucose. In order to evaluate the effect of hydrogenation/dehydrogenation activity on the hexitols yield, the activation energy for glucose hydrogenation was calculated. The glucose hydrogenation was conducted at temperatures of 120–150 °C under 4.0 MPa H<sub>2</sub>. A pseudo-first-order kinetic approximation was assumed for the glucose hydrogenation [29]. It was confirmed that external and internal diffusion was eliminated under the reaction conditions. As summarized in Fig. 4, the activation energy of the Ni/ZSM-5 and Ni/Al<sub>2</sub>O<sub>3</sub> was higher than the activation energy of diffusion in liquids (12–21 kJ mol<sup>-1</sup>) [29], indicating that the reaction rate was controlled by surface reactions. Surprisingly, the activation energy of Ni/Al<sub>2</sub>O<sub>3</sub> was 46.4 kJ mol<sup>-1</sup>, which is lower than that of 54.7 kJ mol<sup>-1</sup> on Ni/ZSM-5. It is estimated that Ni/Al<sub>2</sub>O<sub>3</sub> presented higher activity on glucose hydrogenation than Ni/ZSM-5, which is at variance with the fact that higher yield of hexitols was obtained over Ni/ZSM-5. It indicated that the hydrogenation activity was not sole factor to control the hexitols yield.

In addition, the activation energy of sorbitol dehydrogenation was compared. The dehydrogenation reaction was performed at 220–250 °C under 0.1 MPa N<sub>2</sub>. As shown in Fig. 5, the activation energy on Ni/ZSM-5 and Ni/Al<sub>2</sub>O<sub>3</sub> was 157.4 and 124.3 kJ mol<sup>-1</sup>, respectively. They are much higher than those for hydrogenation, indicating that the dehydrogenation activity was more sensitive to reaction temperature and the rate of dehydrogenation could be promoted greatly with increasing temperature. Additionally, the activation energy on Ni/Al<sub>2</sub>O<sub>3</sub> was about 33 kJ mol<sup>-1</sup> lower than that on Ni/ZSM-5, indicating that the dehydrogenation of hexitols was easier on Ni/Al<sub>2</sub>O<sub>3</sub>, so the yield of hexitols was lower than that on Ni/ZSM-5.

Overall, the production of hexitols was determined by two basic properties—hydrogenation/dehydrogenation activity. The formed hexitols were dehydrogenated and subsequently converted to smaller molecular polyols by retro-aldol condensation, hydrogenation, and dehydration, resulting in lower yield of hexitols; by contrast, higher yield could be obtained over the catalyst with lower dehydrogenation activity. Based on this mechanism, the various catalytic performances of the Ni catalysts could be reasonably explained by the different hydrogenation/dehydrogenation activities. The reason for the yield loss of hexitols on Ni catalysts was proposed as the following two routes: (1) Over the catalyst with inferior hydrogenation activity, the formed glucose was seriously decomposed to complex products by degradation and condensation before hydrogenation; (2) Over the catalyst with high hydrogenation activity, glucose was hydrogenated to hexitols

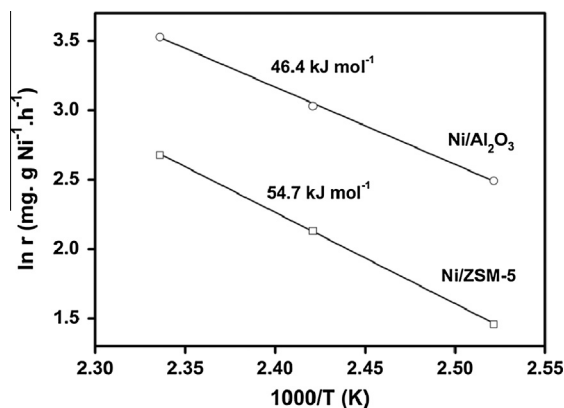


Fig. 4. Arrhenius plot for the hydrogenation of glucose over Ni/ZSM-5 and Ni/Al<sub>2</sub>O<sub>3</sub>. Reaction conditions: 10 mL H<sub>2</sub>O, 4.0 MPa H<sub>2</sub> (RT), glucose 0.5 g, Ni catalyst (17 wt% Ni) 50 mg.

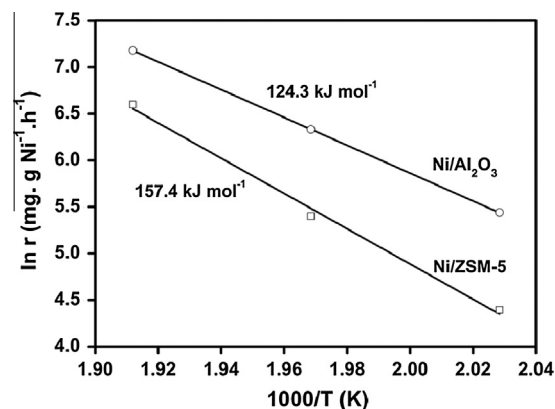


Fig. 5. Arrhenius plot for the dehydrogenation of sorbitol over Ni/ZSM-5 and Ni/Al<sub>2</sub>O<sub>3</sub>. Reaction conditions: 10 mL H<sub>2</sub>O, 4.0 MPa H<sub>2</sub> (RT), glucose 0.5 g, Ni catalyst (17 wt% Ni) 50 mg.

immediately to form hexitols, and the formed hexitols were dehydrogenated into unsaturated species with the catalyst with high dehydrogenation activity either, and then, the subsequently successive reactions, retro-aldol condensation, hydrogenation, and dehydration occurred to yield smaller molecular polyols. For the Ni/kieselguhr catalyst, the route (1) was predominant reaction pathway, resulting in low yield of hexitols. The further hydrogenolysis of hexitols was the predominant reason for the poor yield of hexitols over Ni/Al<sub>2</sub>O<sub>3</sub>, Ni/SiO<sub>2</sub>, Ni/bentonite, and Ni/TiO<sub>2</sub> catalysts in the hydrolytic hydrogenation of cellobiose and glucose. The Ni/ZSM-5 catalyst gave highest yield of hexitols for its high hydrogenation activity and low activity in hexitols dehydrogenation. This implied that we could change the target products or enhance the yield of a specific polyol by turning the hydrogenation/dehydrogenation activity of a catalyst.

### 3.3.3. Surface basicity/acidity and dehydrogenation activity

Very recently, Shimizu et al. reported that  $\gamma$ -Al<sub>2</sub>O<sub>3</sub> showed higher dehydrogenation activity than basic or acidic supports in the dehydrogenation of aliphatic secondary alcohols over supported Pt catalysts, and they discussed the synergistic effect between the Lewis acid–base pair site of alumina and metal site on the dehydrogenation process [37]. Herein, dehydrogenation activities of the catalysts with different surface acidities/basicities

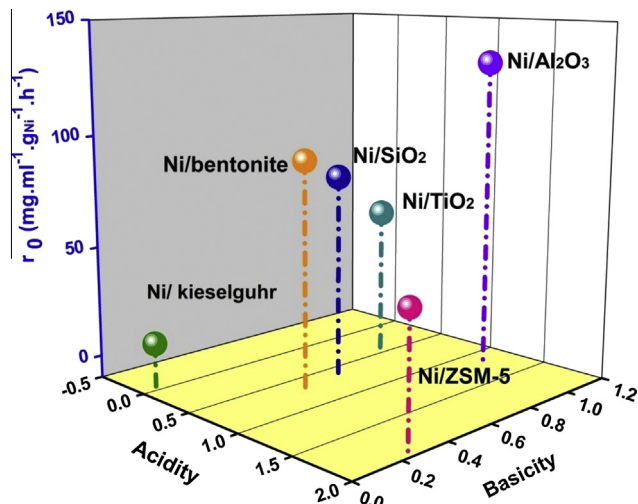


Fig. 6. Effect of surface acidity/basicity of the Ni catalysts on the initial rate for dehydrogenation of sorbitol over various supported Ni catalysts.

**Table 6**  
Results for the hydrogenation of microcrystalline cellulose on different zeolite-supported Ni catalysts.<sup>a</sup>

Catalyst <sup>b</sup>	Conversion (%)	Carbon efficiency (%)	Yield (%)			
			Hexitol	Glycerol	EG	1,2-PDO
Ni/ZSM-5 (38)	83.7	72.3	53.3	3.1	2.4	1.7
Ni/ZSM-5 (50)	85.1	68.5	51.6	2.9	1.8	2.0
Ni/HY (5.6)	82.4	67.8	46.9	3.3	2.1	3.6
Ni/USHY (5.6)	81.5	64.7	44.7	2.9	1.7	3.4

<sup>a</sup> Reaction conditions: 240 °C, H<sub>2</sub> 4.0 MPa (RT), microcrystalline cellulose 0.2 g, H<sub>2</sub>O 10 mL, 4 h, catalyst 100 mg.

<sup>b</sup> Data in parenthesis are Si/Al atom ratio, and Ni loading is 17%.

are illustrated in Fig. 6. The acidity/basicity was estimated, respectively, from the peak area of NH<sub>3</sub>-TPD and CO<sub>2</sub>-TPD profiles (the profiles are shown in Figs. S2 and S3). For CO<sub>2</sub>-TPD, the peak area on Ni/Al<sub>2</sub>O<sub>3</sub> was assigned as 1.0, based on which the surface basicity of other samples was calculated. As shown in Fig. 6, Ni/Al<sub>2</sub>O<sub>3</sub> has stronger acidity and basicity and it gave higher dehydrogenation activity; while the Ni/kieselguhr without acid or base sites gives the lowest dehydrogenation activity. In addition, Ni/ZSM-5 has less base sites among the checked catalysts, and it shows much lower dehydrogenation activity. As well as, Ni/SiO<sub>2</sub>, Ni/bentonite and Ni/TiO<sub>2</sub> have moderate amount of base sites, and they are moderately active in sorbitol dehydrogenation. Therefore, the dehydrogenation is strongly dependence on the surface acidity/basicity of catalyst. This dehydrogenation step resulted in unsaturated adsorbed species, which could be desorbed into bulk solution to form glucose. On the other hand, the unsaturated adsorbed species underwent retro-aldol condensation catalyzed by the acid–base sites of the support or H<sup>+</sup>/OH<sup>-</sup> dissociated by hot-compressed water.

In order to verify this hypothesis, several additional typical zeolites with strong acid sites and weak base sites were tested for the hydrolytic hydrogenation of cellulose. Table 6 shows the catalytic performance over Ni/ZSM-5 (H type, Si/Al 38), Ni/ZSM-5 (H type, Si/Al 50), Ni/HY (Si/Al 5.6), and Ni/USHY (Si/Al 5.6). All the zeolite-supported Ni catalysts gave high carbon efficiency and hexitols yield, which were comparable with that over Ni/ZSM-5 (H type, Si/Al 25). It suggested that the high hydrogenation activity of the Ni nanoparticles was maintained, and moreover, the dehydrogenation of hexitols was still inhibited over these Ni catalysts. All the selected zeolites have large amount of acidic sites, but lack of acid–base pair sites. Thus, the dehydrogenation of hexitol is unavailable on these catalysts resulting in high yield of hexitols.

Based on the kinetic experiments of the dehydrogenation and hydrogenation activity, more knowledge about conversion of cellulose to hexitols over Ni catalysts is gained. First of all, the dehydrogenation of hexitols over Ni catalysts was the crucial step for the hydrogenolysis of hexitols. Besides the excellent hydrogenation activity, the catalyst should have an activation barrier for the dehydrogenation of hexitols, which should be higher than desorption energy of hexitols to favor hexitols desorption rather than the further hydrogenolysis over it. It has been confirmed that the  $\alpha$ -C–H dissociation was the rate-limiting step in dehydrogenation [37]. The activation and dissociation of the  $\alpha$ -C–H of hexitols (sorbitol and mannitol) were related to the *d*-band center of the nickel particles which depended on the surface nickel properties. The electronic state of the Ni particles on various supports was different due to the variation in the arrangement of surface atoms, the metal–support interaction, or the morphology of Ni particles. The further insight over the correlation between the activation energy of the dehydrogenation and the shift of the *d*-band center is under investigation.

#### 4. Conclusion

The basic reaction steps in the hydrolytic hydrogenation of cellulose, including hydrolysis, hydrogenation of cellobiose and glucose, hydrogenolysis of sorbitol, and dehydrogenation of sorbitol were discussed on a series of supported nickel catalysts. At elevated temperature, the hydrogenolysis of hexitols was the primary reason for the loss of hexitols yield over Ni catalysts. We proposed that the hydrogenolysis was started from dehydrogenation followed by retro-aldol condensation and re-hydrogenation. The hydrogenation/dehydrogenation activity of Ni catalysts had crucial effect on hexitols yield. The dehydrogenation of sorbitol was sensitive to temperature and became serious especially at elevated temperatures. The synergistic effect of the Ni site and acid–base site of the support on dehydrogenation of sorbitol was proposed. It is confirmed that the more acidic sites and the relatively less active metal species for C–H dissociation could suppress the dehydrogenation of hexitols and guarantee high yield of hexitols that will be of great importance for designing novel-supported catalysts for the hydrolytic hydrogenation of cellulose to produce high yield of hexitols.

#### Acknowledgments

The authors gratefully acknowledge the financial support from NSFC 21273222 and 20086036, 20100562 from Jilin Provincial Science and Technology Department, China.

#### Appendix A. Supplementary material

Supplementary data associated with this article can be found, in the online version, at <http://dx.doi.org/10.1016/j.jcat.2013.10.022>.

#### References

- [1] S. Van de Vyver, J. Geboers, P. Jacobs, B. Sels, *ChemCatChem* 3 (2011) 82–94.
- [2] A. Ruppert, K. Weinberg, R. Palkovits, *Angew. Chem. Int. Ed.* 51 (2012) 2564–2601.
- [3] G.W. Huber, S. Iborra, A. Corma, *Chem. Rev.* 106 (2006) 4044.
- [4] A. Wang, T. Zhang, *Acc. Chem. Res.* 46 (2013) 1377–1386.
- [5] A. Fukuoka, P.L. Dhepe, *Angew. Chem. Int. Ed.* 45 (2006) 5161.
- [6] C. Luo, S.A. Wang, H.C. Liu, *Angew. Chem. Int. Ed.* 46 (2007) 7636.
- [7] W.P. Deng, M. Liu, X.S. Tan, Q.H. Zhang, Y. Wang, *J. Catal.* 271 (2010) 22.
- [8] J. Geboers, S. Van de Vyver, K. Carpentier, K. de Blochouse, P. Jacobs, B. Sels, *Chem. Commun.* 46 (2010) 3577.
- [9] R. Palkovits, K. Tajvidi, A.M. Ruppert, J. Procelewska, *Chem. Commun.* 47 (2011) 576.
- [10] Y. Liu, C. Luo, H. Liu, *Angew. Chem. Int. Ed.* 51 (2012) 3249.
- [11] R. Palkovits, K. Tajvidi, J. Procelewska, R. Rinaldi, A. Ruppert, *Green Chem.* 12 (2010) 972.
- [12] J. Geboers, S. Van de Vyver, K. Carpentier, P. Jacobs, B. Sels, *Chem. Commun.* 47 (2011) 5590.
- [13] J.A. Geboers, S. Van de Vyver, R. Ooms, B. Op de Beeck, P.A. Jacobs, B.F. Sels, *Catal. Sci. Technol.* 1 (2011) 714.
- [14] W.P. Deng, X.S. Tan, W.H. Fang, Q.H. Zhang, Y. Wang, *Catal. Lett.* 133 (2009) 167.
- [15] G. Liang, C. Wu, L. He, J. Ming, H. Cheng, L. Zhuo, F. Zhao, *Green Chem.* 13 (2011) 839.



- [16] B. Op de Beeck, J. Geboers, S. Van de Vyver, J. Van Lishout, J. Snelders, W. Huijgen, C. Courtin, P. Jacobs, B. Sels, *ChemSusChem* 6 (2013) 199–208.
- [17] N. Ji, T. Zhang, M. Zheng, A. Wang, H. Wang, X. Wang, J.G. Chen, *Angew. Chem. Int. Ed.* 47 (2008) 8510.
- [18] Y.H. Zhang, A.Q. Wang, T. Zhang, *Chem. Commun.* 46 (2010) 862.
- [19] M. Zheng, A.-Q. Wang, N. Ji, J. Pang, X. Wang, T. Zhang, *ChemSusChem* 3 (2010) 63.
- [20] S. Van de Vyver, J. Geboers, M. Dusselier, H. Schepers, T. Vosch, L.A. Zhang, G. Van Tendeloo, P.A. Jacobs, B.F. Sels, *ChemSusChem* 3 (2010) 698.
- [21] S. Van de Vyver, J. Geboers, W. Schutyser, M. Dusselier, P. Eloy, E. Dornez, J. Seo, C. Courtin, E. Gaigneaux, P. Jacobs, B. Sels, *ChemSusChem* 5 (2012) 1549–1558.
- [22] L.N. Ding, A.Q. Wang, M.Y. Zheng, T. Zhang, *ChemSusChem* 3 (2010) 818.
- [23] J. Pang, A. Wang, M. Zheng, Y. Zhang, Y. Huang, X. Chen, T. Zhang, *Green Chem.* 14 (2012) 614.
- [24] Z. Tai, J. Zhang, A. Wang, J. Pang, M. Zheng, T. Zhang, *ChemSusChem* 6 (2013) 652–658.
- [25] X. Wang, L. Meng, F. Wu, Y. Jiang, L. Wang, X. Mu, *Green Chem.* 14 (2012) 758.
- [26] G. Liang, H. Cheng, W. Li, L. He, Y. Yu, F. Zhao, *Green Chem.* 14 (2012) 2146.
- [27] S. Velu, S. Gangwal, *Solid State Ionics* 177 (2006) 803.
- [28] A. Shrotri, A. Tanksale, J. Beltramini, H. Gurav, S. Chilukuric, *Catal. Sci. Technol.* 2 (2012) 1852.
- [29] N. Dechamp, A. Gamez, A. Perrard, P. Gallezot, *Catal. Today* 24 (1995) 29.
- [30] V. Jollet, F. Chambon, F. Rataboul, A. Cabiac, C. Pinel, E. Guillon, N. Essayem, *Green Chem.* 11 (2009) 2052.
- [31] H. Kobayashi, Y. Ito, T. Komanoya, Y. Hosaka, P.L. Dhepe, K. Kasai, K. Hara, A. Fukuoka, *Green Chem.* 13 (2011) 326.
- [32] I. Baek, S. You, E. Park, *Bioresour. Technol.* 114 (2012) 684.
- [33] S. Schimpf, C. Louis, P. Claus, *Appl. Catal. A* 318 (2007) 45.
- [34] P. Gallezot, P.J. Cerino, B. Blanc, G. Flèche, P. Fuertes, *J. Catal.* 146 (1994) 93–102.
- [35] B. Kusserow, S. Schimpf, P. Claus, *Adv. Synth. Catal.* 345 (2003) 289.
- [36] J. Sun, H. Liu, *Green Chem.* 13 (2011) 135.
- [37] K. Kon, H. Siddiki, K. Shimizu, *J. Catal.* 304 (2013) 63.